SPRFMO

5th Meeting of the Scientific Committee

Shanghai, China, 23 - 28 September 2017

SC5-SQ06

Impacts of Climate variability on habitat suitability of Jumbo flying squid in the Southeast Pacific Ocean off Peruvian waters

Wei Yu, Xinjun Chen & Yong Chen

Impacts of climate variability on habitat suitability of jumbo flying squid *Dosidicus gigas* in the Southeast Pacific Ocean off Peruvian waters

Wei Yu, Xinjun Chen, Yong Chen

National Data Center for Distant-water Fisheries, Shanghai Ocean University

1. Introduction

The jumbo flying squid, *Dosidicus gigas*, is a large active squid with an extensive coastal and oceanic range between 40°N and 47°S throughout the Eastern Pacific Ocean (Nigmatullin *et al*., 2001). As a commercially important species, *D. gigas* sustains major fisheries in the Gulf of California (Morales-Bojórquez and Nevárez-Martínez, 2010), the coastal and oceanic waters of Peru and Chile (Keyl *et al*., 2010), the offshore regions of the Costa Rica Dome (Chen *et al*., 2014), with an exploitation extending westward as far to 120°W at the equator (Liu *et al*., 2015). Multinational jigging vessels from East Asia-Pacific countries have been attracted into the *D. gigas* fisheries in the Eastern Pacific Ocean (Ichii *et al*., 2002). Among them, Chinese squid-jigging fishing vessels began to survey this squid in 2001 outside the exclusive economic zone (EEZ) off Peru, and subsequently developed a large squid fishery across the Southeast Pacific and kept high levels of catches of *D. gigas* in recent years (Chen *et al*., 2008a).

Dosidicus gigas has become the largest fishery among the world squid fisheries (Rocha and Vega, 2003). Understanding the process that *D. gigas* habitat reacts to the climate variability is an essential step towards better fisheries management. It is urgent to conduct a habitat assessment for *D. gigas*. However, to our knowledge, the interaction between the habitat of *D. gigas* and large-scale climate change is unknown and has not yet been examined in recent decadal years. Here, we apply a HSI model to time-series of *D. gigas* on the fishing ground in the Southeast Pacific Ocean off Peru to extract the main features of variability in the spatial distribution of suitable habitat. This HSI model involves with three environmental variables including SST, Chla and SSHA which are strongly correlated to squid abundance. The purposes of this study are (1) to quantify the relationship between the key environmental variables and the spatial distribution of *D. gigas*; (2) to characterize and identify the squid suitable habitat over times; (3) and most importantly to evaluate the impacts of large-scale climate variability (El Niño and La Niña events) on the variations of the optimal habitat and explore the potential mechanism.

2. Materials and methods

2.1. Fishery and environmental data

The fishery data of *D. gigas* on the fishing ground between 8°−20°S and 95°−75°W were available from the Chinese Squid-jigging Technology Group of Shanghai Ocean University, the spatial resolution was 0.5°×0.5° latitude/longitude grid. Fishing operations were performed outside the EEZ off Peru. The fishing date was from January 2006 to December 2013 with a temporal resolution in month. Data information included catch (tons), fishing effort (in fishing days) and fishing location (latitude and longitude).

The monthly SST and SSHA data were sourced from the Live Access Server of National Oceanic and Atmospheric Administration OceanWatch. The monthly MODIS Chla data were obtained from the Asia-Pacific Data-Research Center (APDRC), University of Hawaii. The spatial resolution was 0.1°×0.1° and 0.05°×0.05°, respectively, for AVHRR SST and MODIS Chla data. Before we compiled the environmental data into analysis, the data were averaged on a 0.5°×0.5° latitude/longitude grid to match the fishery data. The definition for El Niño and La Niña events was based on the 3 month running mean of SST anomalies in the Niño 3.4 region (5°N−5°S, 120°−170°W). The Oceanic Niño 3.4 index over 2006−2013 was achieved from the NOAA Climate Prediction Center. The El Niño and La Niña events were measured by the SSTs above or below a threshold of +/- 0.5°C over at least 5 consecutive months, respectively.

2.2. Developing the HSI model

2.2.1. Suitability index

The first step in developing the HSI model was to determine the suitability index (SI), which quantified the probability of species availability. The correlations between the environmental variables and fishing effort as well as the CPUE were both suggested to be good proxies for developing SI models (Chen *et al*., 2010), however, fishing effort tended to yield better model performance (Tian *et al*., 2009). Thus, we employed the fishing effort to calculate the SI values for *D. gigas*. In this study, we divided SST, Chla concentration and SSHA into several segments based on intervals of 1.0°C, 0.1 mg/m^3 and 2 cm on the fishing ground, respectively. The SI values during January to December were created by the ratio of total fishing efforts at a given segment range of environmental variables to the maximum of the total fishing efforts (Li *et al*., 2014).

The SI values ranged from 0 to 1. The highest SI value (SI=1) indicated that the fishing effort in a given interval of environmental variables was maximum, implying that the fishing ground was the most productive habitat for *D. gigas*; while the SI=0 represented the fishing ground was likely to be the poorest habitat with the lowest fishing efforts (Li *et al*., 2014).

The observed SI values based on the equation (2) were then included to develop SI models combined with each class interval value for each environmental variable. We fitted SI models of SST, Chla and SSHA in the form of:

$$SI_{Chla} = a\exp\left[b(Chla-c)^2\right] \quad (1)$$

$$SI_{SST} = \exp\left[b(SST-c)^2\right] \quad (2)$$

$$SI_{SSHA} = \exp\left[b(SSHA-c)^2\right] \quad (3)$$

where a, b and c were the model parameters to be estimated; *Chla*, *SST* and *SSHA* were the class interval values of each environmental variable. We assumed SI=0.6 as the threshold value that defined the suitable range of each environmental variable for *D. gigas* (Yu *et al*., 2015).

2.2.2. Structure the HSI model

An integrated HSI model combined all the significant environmental variables to describe the suitability of a given habitat of species. We structured the integrated HSI model by two empirical algorithms: one was the arithmetic mean HSI model (AMM) (Chang *et al*., 2013) and the other was the geometric mean HSI model (GMM) (Tomsic *et al*., 2007). Both models had been frequently used to estimate the habitat suitability. The equations were described as:

$$HSI_{AMM} = \frac{SI_{Chla} + SI_{SST} + SI_{SSHA}}{3} \quad (4)$$

$$HSI_{GMM} = \sqrt[3]{SI_{Chla} \times SI_{SST} \times SI_{SSHA}} \quad (5)$$

where SI_{Chla} was suitability value for Chla concentration; SI_{SST} was suitability value for SST; SI_{SSHA} was suitability value for SSHA. Fishery and remote sensing environmental data over 2006−2012 were used for HSI modeling. The HSI model output values from 0 to 1 as well, the fishing grounds with HSI value to be equal or greater than 0.6 were considered as optimally suitable habitat for *D. gigas* in the Southeast Pacific Ocean off Peru (Tian *et al*., 2009).

2.2.3. HSI model selection and validation

All the HSI values were clustered into five HSI groups, they were from 0.0 to 0.2, from 0.2 to 0.4, from 0.4 to 0.6, from 0.6 to 0.8 and from 0.8 to 1.0, respectively. We compared the percentage of total catches and fishing efforts in each HSI group obtained from AMM-based and GMM-based HSI models from January to December during 2006−2012. A good HSI model would yield a high consistency between the optimally suitable habitat with HSI>=0.6 and productive catches and fishing efforts, lower percentages of catches and fishing efforts would occur in poor habitat with HSI<=0.4 (Li *et al*., 2014). On that basis, we were prompted to compare and select a better HSI model to predict the habitat suitability.

Moreover, environmental data in 2013 were used to predict the spatial distribution of HSI values by the AMM and GMM models for each month, fishing effort frequencies were then overlain on the predicted HSI maps to test and validate the HSI models. Both the procedure of HSI model selection and validation help us ultimately choose a more suitable HSI model to evaluate the impacts of climate variability on habitat suitability for *D. gigas* on the fishing ground off Peru.

2.3. Evaluating the impacts of climate variability on habitat suitability

Annual spatial and temporal distributions of HSI values over 2006−2012 were predicted by the suitable HSI model we selected. We then evaluate the impacts of ENSO events on habitat suitability by the following steps:

(1) Correlation analysis was conducted between the latitudinal gravity center of fishing effort (LATG) and the average latitude of the areas with the HSI>=0.6 on the fishing ground of *D. gigas* (Chen *et al*., 2012), we attempted to examine how the fishing locations varied with the suitable habitat of *D. gigas*.

(2) Monthly HSI values on the fishing ground were averaged during 2006−2012. In order to identify the variability of the HSI, we smoothed the monthly average HSI values with a 3-month running mean filter and compared with the Niño 3.4 index. To determine whether or not there were time-lagged effects of ENSO events on the squid habitat, the relationship between the average HSI values and the Niño 3.4 index was further explored using cross-correlation plots, with a significance level of $P<0.05$ for time-lags of months (Postuma and Gasalla, 2010).

(3) During 2006−2012, two El Niño (September 2006−January 2007 and July 2009−April 2010) and five La Niña events (January 2006−March 2006, August 2007−June 2008, November

2008−March 2009, July 2010−April 2011 and August 2011−March 2012) were observed (Table 1). Fishing months from January to March in 2006, 2008−2012 and from September to December in 2006, 2007, 2009−2011 were chosen as our study periods in this section, because all the selected fishing months in these years above-mentioned corresponded to an anomalous environmental event (El Niño/ La Niña) (Table 1). Monthly HSI contour maps were created, as well as the evaluation of the suitable habitat areas (defined by the total fishing units with HSI>=0.6 occupying the waters on the fishing ground) and total catches for each month.

Table 1. The Oceanic Niño Index in the Niño 3.4 region (5ºN−5ºS, 120º−170ºW). Blue shading indicates La Niña events occurs; red shading indicates El Niño events occurs; green shading indicates normal climate condition, with box indicating the fishing periods we selected to evaluate the impacts of climate variability on the habitat suitability for the jumbo flying squid *Dosidicus gigas* in the Southeast Pacific Ocean.

	Jan	Feb	Mar	Apr	May	Jun	Jul	Aug	Sep	Oct	Nov	Dec
2006	-0.9	-0.7	-0.5	-0.3	0.0	0.1	0.2	0.3	0.5	0.8	1.0	1.0
2007	0.7	0.3	-0.1	-0.2	-0.3	-0.3	-0.4	-0.6	-0.8	-1.1	-1.2	-1.4
2008	-1.5	-1.5	-1.2	-0.9	-0.7	-0.5	-0.3	-0.2	-0.1	-0.2	-0.5	-0.7
2009	-0.8	-0.7	-0.5	-0.2	0.2	0.4	0.5	0.6	0.8	1.1	1.4	1.6
2010	1.6	1.3	1.0	0.6	0.1	-0.4	-0.9	-1.2	-1.4	-1.5	-1.5	-1.5
2011	-1.4	-1.2	-0.9	-0.6	-0.3	-0.2	-0.2	-0.4	-0.6	-0.8	-1.0	-1.0
2012	-0.9	-0.6	-0.5	-0.3	-0.2	0.0	0.1	0.4	0.5	0.6	0.2	-0.3

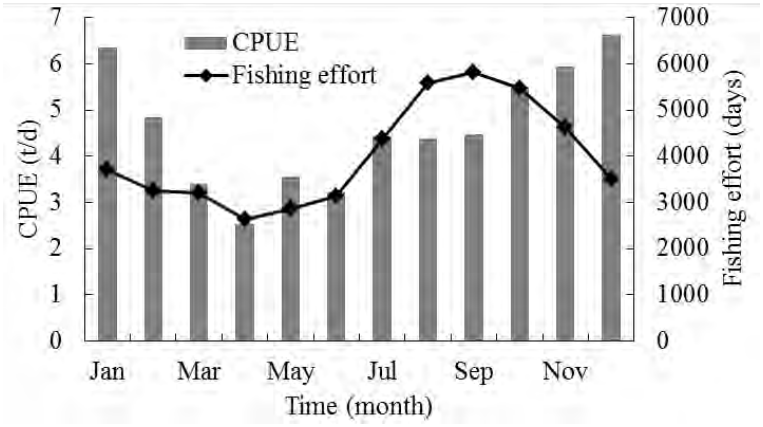

Figure 1. Monthly CPUE of *Dosidicus gigas* and fishing effort during 2006−2013.

3. Results

3.1. Seasonal variability of CPUE and fishing effort of *D. gigas*

There was significant seasonal variability in the CPUE and fishing effort of *D. gigas* in the Southeast Pacific Ocean off Peru (Fig. 1). Both gradually decreased from January to March and then increased from April to December. CPUE was high in July to February, it ranged from 4.40 to 6.64 t/d. The lowest CPUE occurred in April with the value of 2.52 t/d. High frequencies of fishing effort were found through July to December. However, the fishing efforts tended to be relatively low from April to June.

3.2. Suitability index of environmental variables

The SI models were established in Table 2 for each environmental variable (SST, Chla and SSHA) during January to December. Statistical analyses for these SI models were all significant (P<0.05) mostly with high correlation coefficients of the spline smooth regression models. The optimal range of each environmental variable varied with the fishing month (Fig. 2). For example, the suitable range of SST tended to be high from January to May, and low from July to December. The monthly suitable range of SSHA was generally from -4 cm to 2 cm, most of fishing efforts occurred in waters with SSHA below 0, it subjected to small changes. For Chla, we found that the suitable range exhibited the opposite trend as the variability of SST, was typically low in the early fishing months from January to June but high in the following months. It was observed that the high SI mainly occupied the suitable range of Chla concentration between 0.15 mg/m^3 and 0.25 mg/m^3 from January to August, and between 0.25 mg/m^3 and 0.35 mg/m^3 from September to December, respectively.

Table 2. Estimation of statistical parameters for the suitability index (SI) model for each

environmental variable included in this study during January to December.

Month	SI model	R^2	F	P
January	$SI_{SST} = \exp(-0.8251(X_{SST} - 22.8197)^2)$	0.9991	6541.198	0.0001
	$SI_{SSHA} = \exp(-0.1101(X_{SSHA} - 0.0551)^2)$	0.5737	9.4198	0.0181
	$SI_{Chla} = 1.0555\exp(-56.6238(X_{Chla} - 0.195)^2)$	0.9631	26.0976	0.0369
February	$SI_{SST} = \exp(-0.7947(X_{SST} - 24.3268)^2)$	0.9733	145.8186	0.0003
	$SI_{SSHA} = \exp(-0.2797(X_{SSHA} + 3.4198)^2)$	0.5754	10.8426	0.0110
	$SI_{Chla} = 1.1536\exp(-166.924(X_{Chla} - 0.1707)^2)$	0.9987	750.7286	0.0013
March	$SI_{SST} = \exp(-0.2402(X_{SST} - 24.5679)^2)$	0.8829	45.2241	0.0005
	$SI_{SSHA} = \exp(-0.1075(X_{SSHA} + 2.4087)^2)$	0.8818	52.2429	0.0002
	$SI_{Chla} = 1.1843\exp(-80.2778(X_{Chla} - 0.1418)^2)$	0.9921	250.0701	0.0001
April	$SI_{SST} = \exp(-0.1640(X_{SST} - 23.4536)^2)$	0.5064	8.2061	0.0210
	$SI_{SSHA} = \exp(-0.1179(X_{SSHA} + 1.0711)^2)$	0.9455	121.3608	0.0001
	$SI_{Chla} = 1.1383\exp(-118.99(X_{Chla} - 0.1356)^2)$	0.9665	43.3134	0.0061
May	$SI_{SST} = \exp(-0.3663(X_{SST} - 21.5533)^2)$	0.9454	86.6263	0.0002
	$SI_{SSHA} = \exp(-0.043(X_{SSHA} + 1.5829)^2)$	0.8666	58.4615	0.0001
	$SI_{Chla} = 1.0934\exp(-77.9105(X_{Chla} - 0.1717)^2)$	0.9862	178.0801	0.0001
June	$SI_{SST} = \exp(-0.3109(X_{SST} - 20.0884)^2)$	0.8870	54.9234	0.0001
	$SI_{SSHA} = \exp(-0.0949(X_{SSHA} - 0.4362)^2)$	0.5582	10.1072	0.0130
	$SI_{Chla} = 1.217\exp(-99.0105(X_{Chla} - 0.15)^2)$	0.9510	48.5682	0.0005
July	$SI_{SST} = \exp(-0.3951(X_{SST} - 18.4135)^2)$	0.9198	80.2579	0.0001
	$SI_{SSHA} = \exp(-0.1172(X_{SSHA} - 0.0541)^2)$	0.8980	70.402	0.0001
	$SI_{Chla} = 1.0239\exp(-111.581(X_{Chla} - 0.1854)^2)$	0.9998	7710.1	0.0001
August	$SI_{SST} = \exp(-0.4938(X_{SST} - 17.5014)^2)$	0.6941	15.8867	0.0053
	$SI_{SSHA} = \exp(-0.0624(X_{SSHA} + 0.6123)^2)$	0.9817	376.542	0.0001
	$SI_{Chla} = 1.0835\exp(-184.366(X_{Chla} - 0.1791)^2)$	0.9935	381.7112	0.0001
September	$SI_{SST} = \exp(-0.2218(X_{SST} - 17.6917)^2)$	0.7979	23.6932	0.0028
	$SI_{SSHA} = \exp(-0.05(X_{SSHA} + 1.1077)^2)$	0.8359	35.6653	0.0006
	$SI_{Chla} = 1.0111\exp(-65.9128(X_{Chla} - 0.2308)^2)$	0.9747	57.7715	0.0040
October	$SI_{SST} = \exp(-1.7642(X_{SST} - 18.8701)^2)$	0.6530	9.4104	0.0279
	$SI_{SSHA} = \exp(-0.0796(X_{SSHA} + 0.3239)^2)$	0.7859	29.3702	0.0006
	$SI_{Chla} = 0.9997\exp(-156.92(X_{Chla} - 0.1992)^2)$	0.9934	451.2811	0.0001
November	$SI_{SST} = \exp(-0.3425(X_{SST} - 18.9916)^2)$	0.8424	26.7224	0.0036
	$SI_{SSHA} = \exp(-0.0475(X_{SSHA} + 1.1748)^2)$	0.8889	55.992	0.0001
	$SI_{Chla} = 1.0214\exp(-77.3996(X_{Chla} - 0.2234)^2)$	0.9908	214.9652	0.0001
December	$SI_{SST} = \exp(-0.4509(X_{SST} - 20.2035)^2)$	0.9745	191.4517	0.0001
	$SI_{SSHA} = \exp(-0.0676(X_{SSHA} + 1.9897)^2)$	0.9596	190.1979	0.0001

$SI_{Chla} = 1.1225\exp(-72.2077(X_{Chla} - 0.2398)^2)$	0.9998	8121.24	0.0001

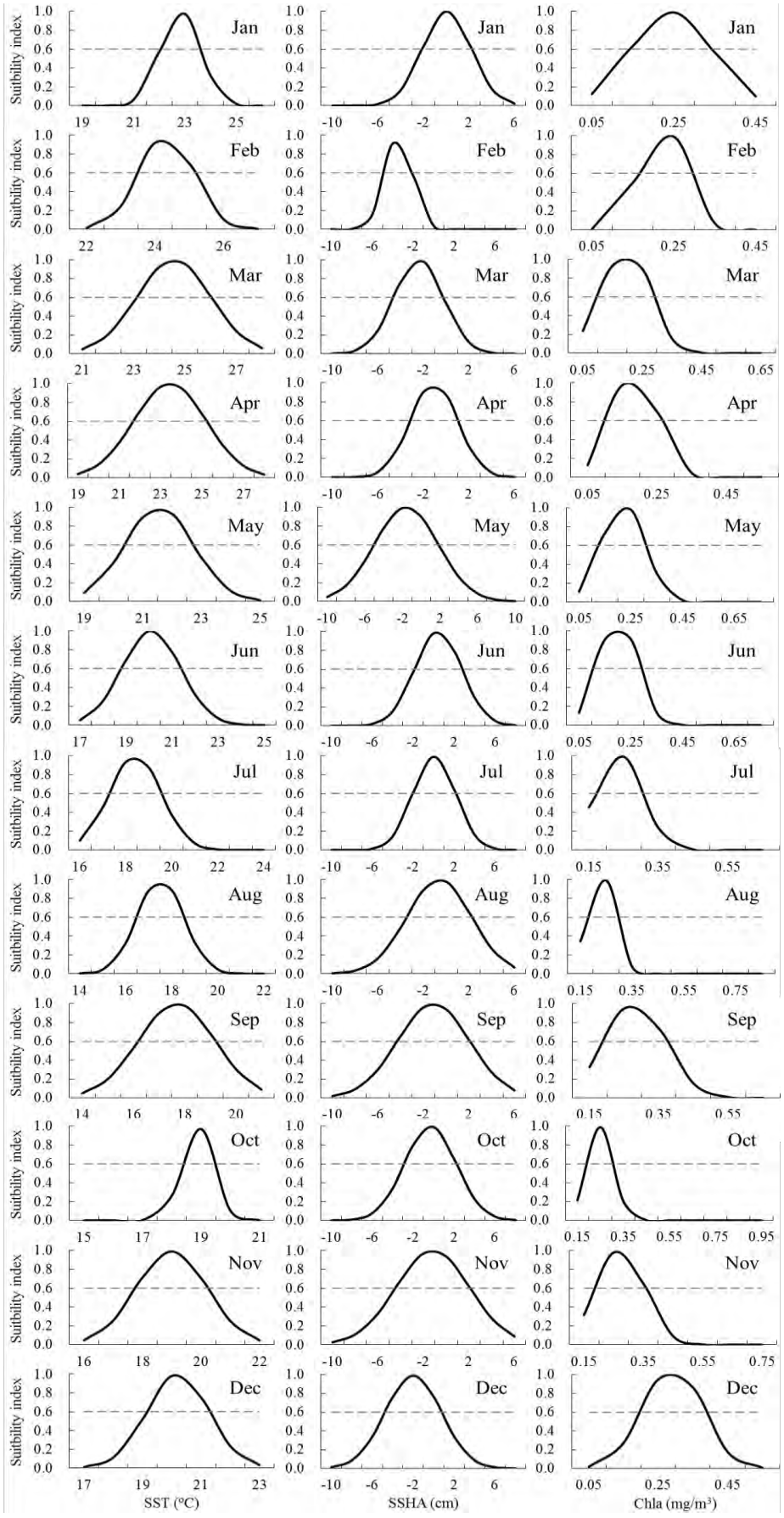

Figure 2. The monthly estimated suitability index (SI) curve for sea surface temperature (SST), sea surface height anomaly (SSHA) and sea surface chlorophyll-a (Chla) for *Dosidicus gigas* derived from the spline smooth regression method. The interactions between the SI curves and the dashed line (SI=0.6) determined the optimal range of each environmental variable in each month.

3.3. Comparison between AMM-based and GMM-based HSI models

We observed that the AMM-based and GMM-based HSI models yielded obviously different model performances by examining the percentage of total catches and fishing efforts in each stratum of HSI values (Fig. 3). In general, a small proportion of catches and fishing efforts occupied the fishing grounds with the HSI between 0.0 and 0.2 and between 0.2 and 0.4 from the two HSI models, larges proportions occurred in the habitat with the HSI higher than 0.4, especially higher than 0.6. However, great differences were also found for the distributions of catch and fishing effort in relation to the HSI values. First, for the poorest habitat within the HSI class range between 0.0−0.2, the AMM-based HSI model attracted much smaller proportions of catches and fishing efforts comparing to the results from the GMM-based HSI model. Taking the fishing months in February, April, June, August and October for example, the percentages of catches from the AMM model were 3.81%, 0.00%, 0.22%, 0.75% and 9.95%, respectively, corresponding to extremely higher percentages of 54.13%, 11.19%, 22.11%, 16.63% and 51.11% from the GMM model. Similarly, based on the AMM-based HSI model, the percentages of fishing effort were 3.86%, 0.00%, 0.22%, 0.79% and 9.14%, respectively, which were much lower than those of 54.77%, 13.31%, 23.16%, 13.48% and 48.33%, respectively, according to the AMM-based HSI model in these months. Second, for the common habitat with the HSI range of 0.4−0.6, it was notable that the AMM model mainly yielded more productive catches and higher fishing efforts than those by the GMM model. Finally, for the optimally suitable habitat within the HSI class range of 0.6−1.0, the total catch and fishing effort all contributed higher proportions by the AMM model than those for the GMM model. Through the comparison, the results suggested that the AMM-based HSI model was more appropriate to predict the squid habitat suitability than the GMM-based HSI model due to a better model performance.

3.4. HSI model validation

We used both the AMM and GMM methods to make a prediction of the spatial distribution of HSI values from January to December in the Southeast Pacific Ocean off Peru (Fig. 4). It was found that the HSI values estimated from the AMM model were higher than those from the GMM model, as well as the area of suitable habitat. In addition, most of fishing locations were observed to be distributed in the regions with HSI>=0.6 according to the AMM model. However, with respect to the GMM model, there were considerable fishing sites locating in the areas with relatively low HSI, such as large numbers of fishing efforts occurred in the northern waters during February and March and southern waters in October off Peru. These findings further confirmed our conclusion that the AMM model was better than the GMM model for predicting the HSI values. Thus, we applied the AMM-based model to predict the habitat suitability of *D. gigas* over 2006−2012 in the subsequent sections.

3.5. Distribution of fishing efforts in relation to squid suitable habitat

During 2006−2012, the LATG greatly fluctuated ranging from 10.5°S in July 2007 to 19.1°S in April 2012, with relatively small variability in 2006 and 2011 (Fig. 5). Distribution of fishing efforts also performed seasonal migrations in each year. Annual LATG initially moved southward during the early fishing months and then shifted northward in the following months. Similar to the LATG with identical migration pattern, the annual average latitude of areas with HSI>=0.6 varied from 13.5°S in January 2008 to 16.7°S in April 2008. Correlation analysis suggested that a statistically significant positive relationship existed between the annually average latitude of suitable habitat and the LATG (R=0.453, P<0.001).

3.6. Relationship between the Niño 3.4 index and habitat quality

The average HSI value on the fishing ground was used to describe the habitat quality for *D. gigas*. It ranged from 0.38 in February 2010 to 0.74 in November 2010 and tended to be in high frequency variability (Fig. 6). We used a 3-month running mean filter to smooth this time-series data and compared with the Niño 3.4 index. High average HSI values were found to coincide with low Niño 3.4 index. The cross-correlation analysis suggested a significantly negative relationship was between the average HSI values and Niño 3.4 index at a time lag of -1−3 months, the highest correlation occurred at a 2-month time lag with a coefficient value of -0.31 (Fig. 7).

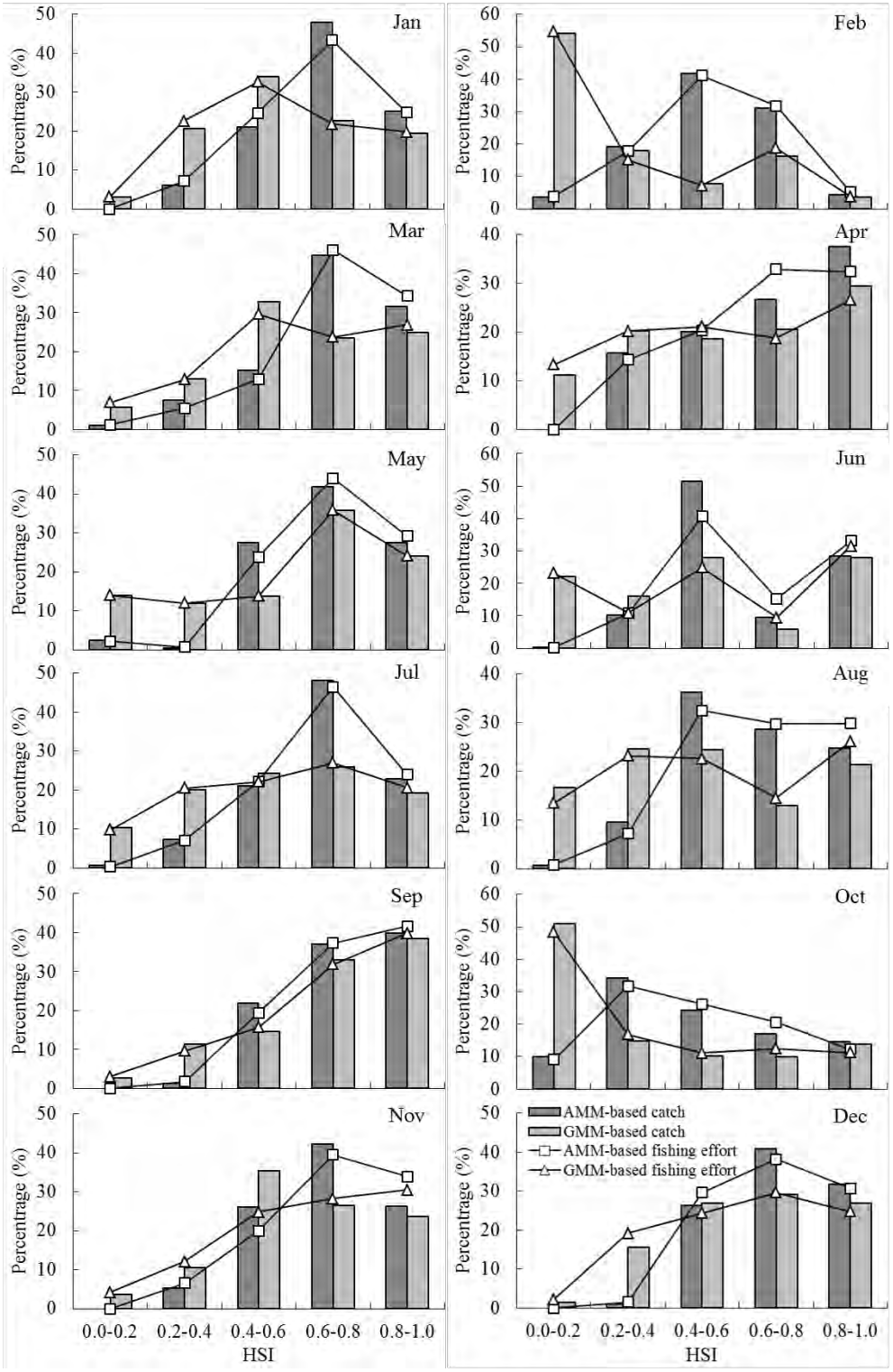

Figure 3. Comparing the frequency of catch and fishing effort within each habitat suitability index (HSI) stratum estimated from the arithmetic mean model (AMM) and the geometric mean model (GMM) for each month.

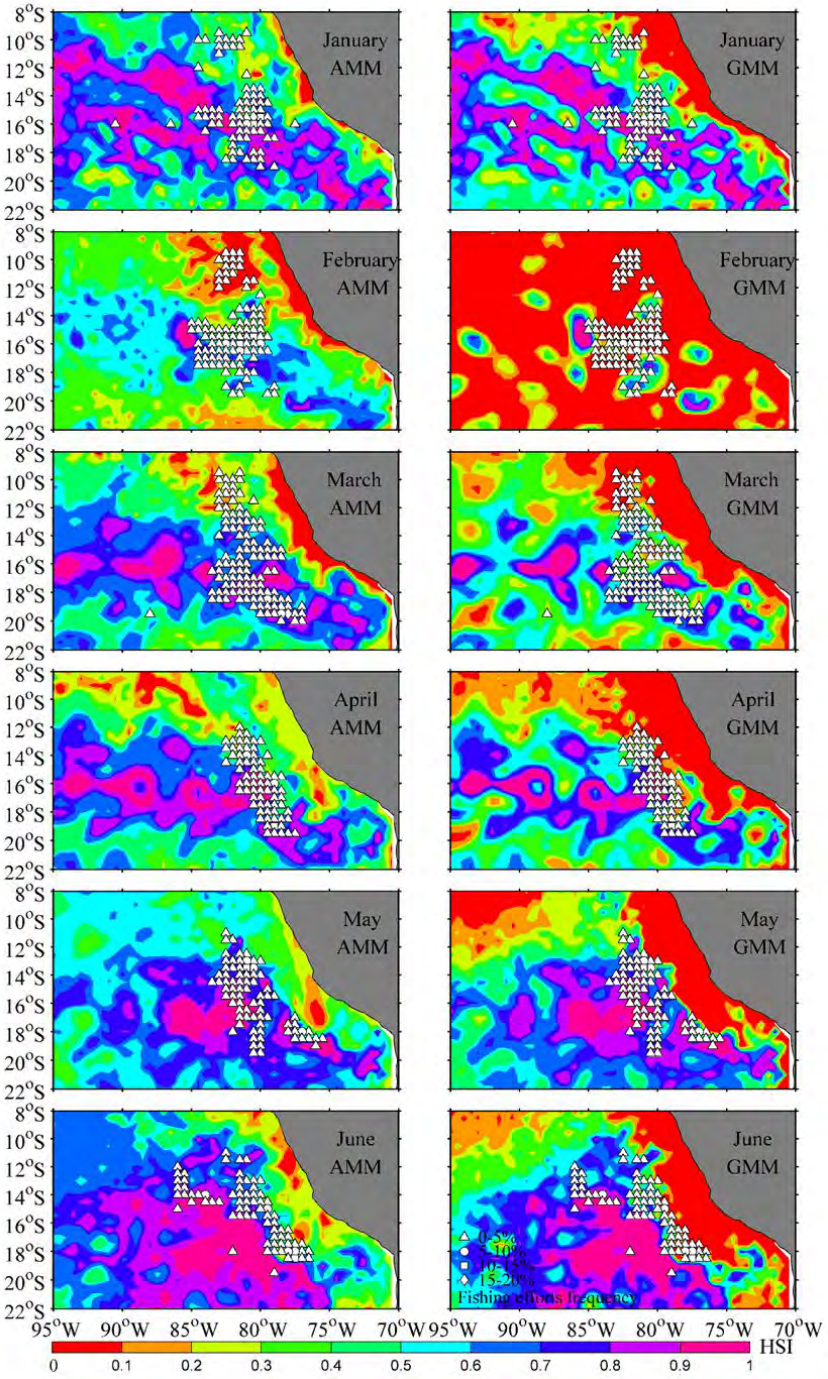
January AMM
January GMM
February AMM
February GMM
March AMM
March GMM
April AMM
April GMM
May AMM
May GMM
June AMM
June GMM
8°S
10°S
12°S
14°S
16°S
18°S
20°S
22°S
95°W 90°W 85°W 80°W 75°W 70°W
0-5%
5-10%
10-15%
15-20%
Fishing effort frequency
HSI
0 0.1 0.2 0.3 0.4 0.5 0.6 0.7 0.8 0.9 1

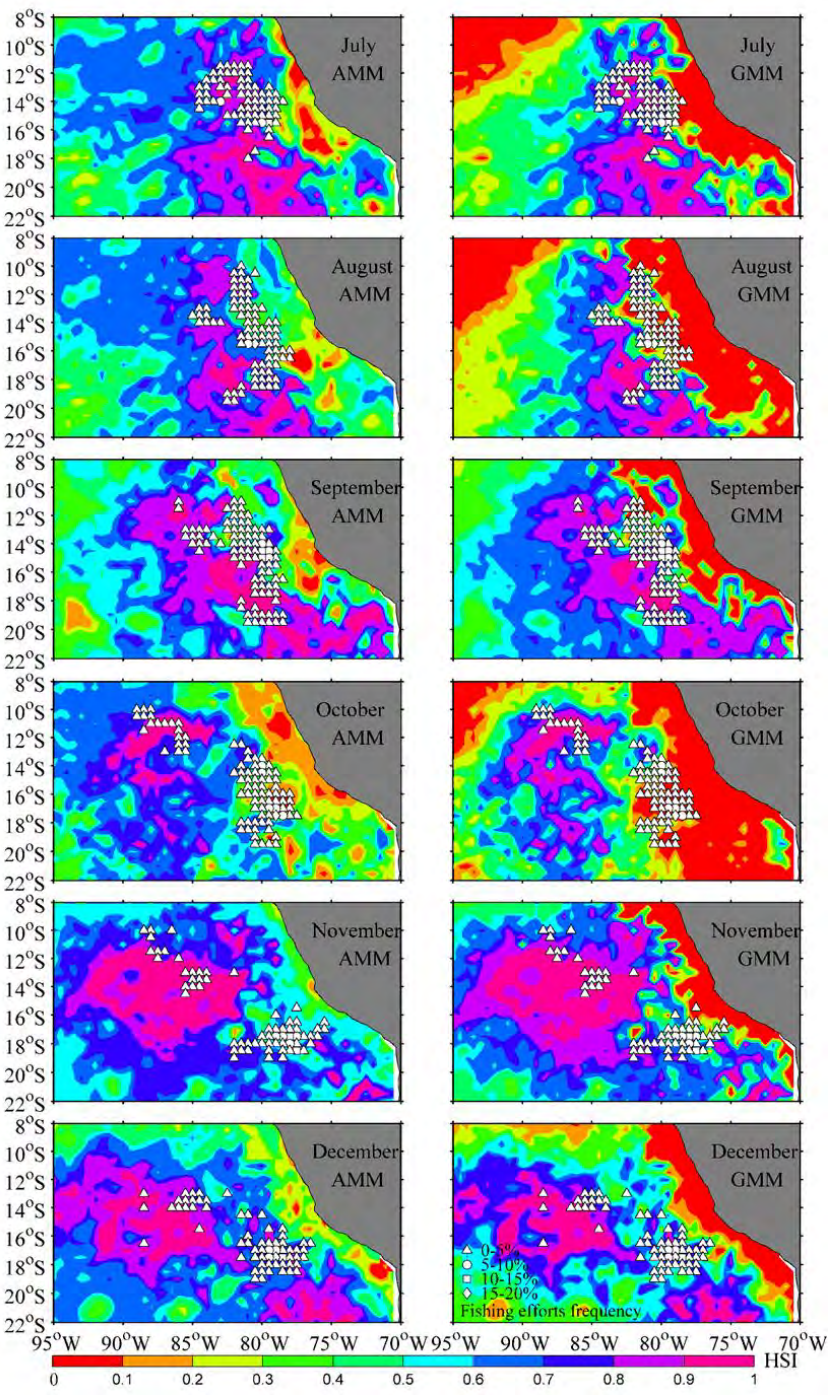

Figure 4. Comparing the spatial distribution of fishing effort frequency superimposed on the predicted HSI values from January to December in 2013 derived from AMM-based and GMM-based HSI models.

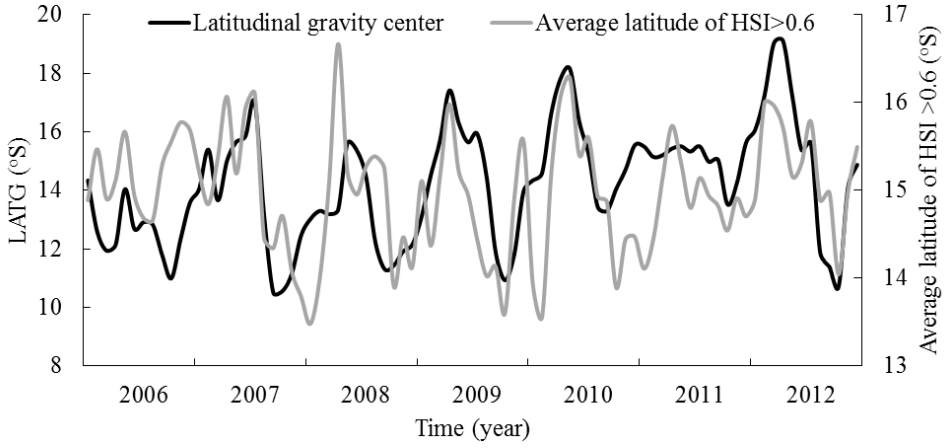

Figure 5. The relationship between the latitudinal gravity centers of fishing effort and the average latitude of HSI values above 0.6.

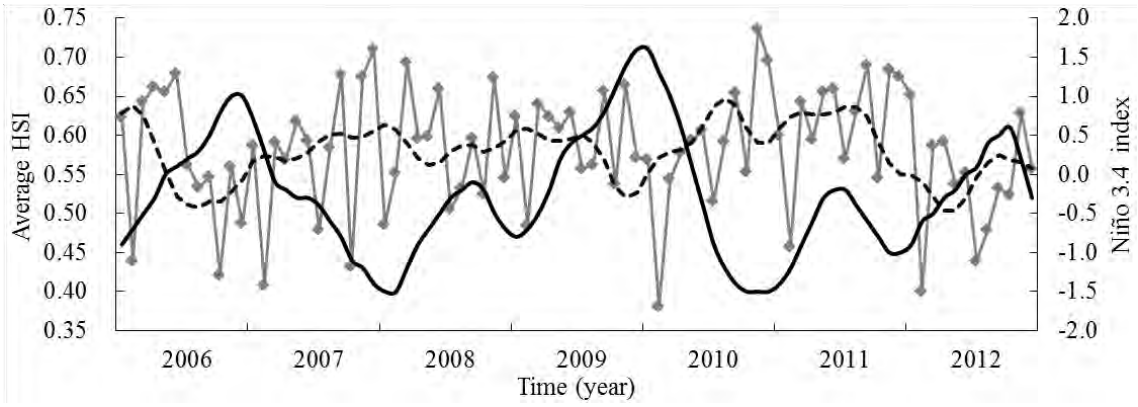

Figure 6. The relationship between the average HSI values on the fishing ground of *Dosidicus gigas* and the Niño 3.4 index over 2006−2012. The grey line denoted the average HSI values on the fishing ground by the Chinese squid-jigging fishery for *Dosidicus gigas*. The black dashed line denoted the 3 month running mean of average HSI values. The black solid line denoted the Niño 3.4 index from 2006 to 2012.

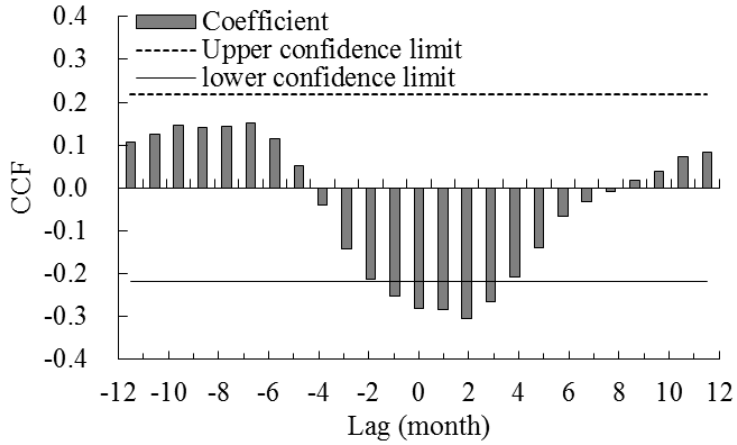

Figure 7. Estimated cross-correlation with the time lags between significantly correlated average HSI values and the Niño 3.4 index during 2006−2012.

3.7. Variability in suitable habitat area and catch of *D. gigas* corresponding to different ENSO events

Figure 8 showed the contour maps of the spatial distribution of HSI values for *D. gigas* during January to March in 2006 and 2008−2012. We found that the predicted favorable habitats in January and March were larger than those in February. Comparing the squid habitat for each month, the suitable habitat tended to be shrunken in January 2008, February 2010 and 2012 and March 2010. We then conducted quantitative analyses of potential *D. gigas* habitats, from January to March, the suitable habitats occupied the total fishing cells from 259 to 603 cells in 2006 with a La Niña event, from 269 to 699 cells in 2008 with a La Niña event, from 364 to 626 cells in 2009 with a La Niña event, from 152 to 488 cells in 2010 with an El Niño event, from 340 to 629 cells in 2011 with a La Niña event and from 196 to 642 cells in 2012 with a La Niña event, respectively (Fig. 9). It was suggested the habitat was unfavorable for the squid growth in 2010 because of a large decrease in the areas of suitable habitat. Such variability directly influenced the catch of *D. gigas*, leading to an extremely low catch in 2010 with 894 t in January, 906 t in February and 867 t in March (Fig. 9). However, the catch in other fishing months was basically higher than 1000 t, the largest catch was even up to 4153 t in January 2011.

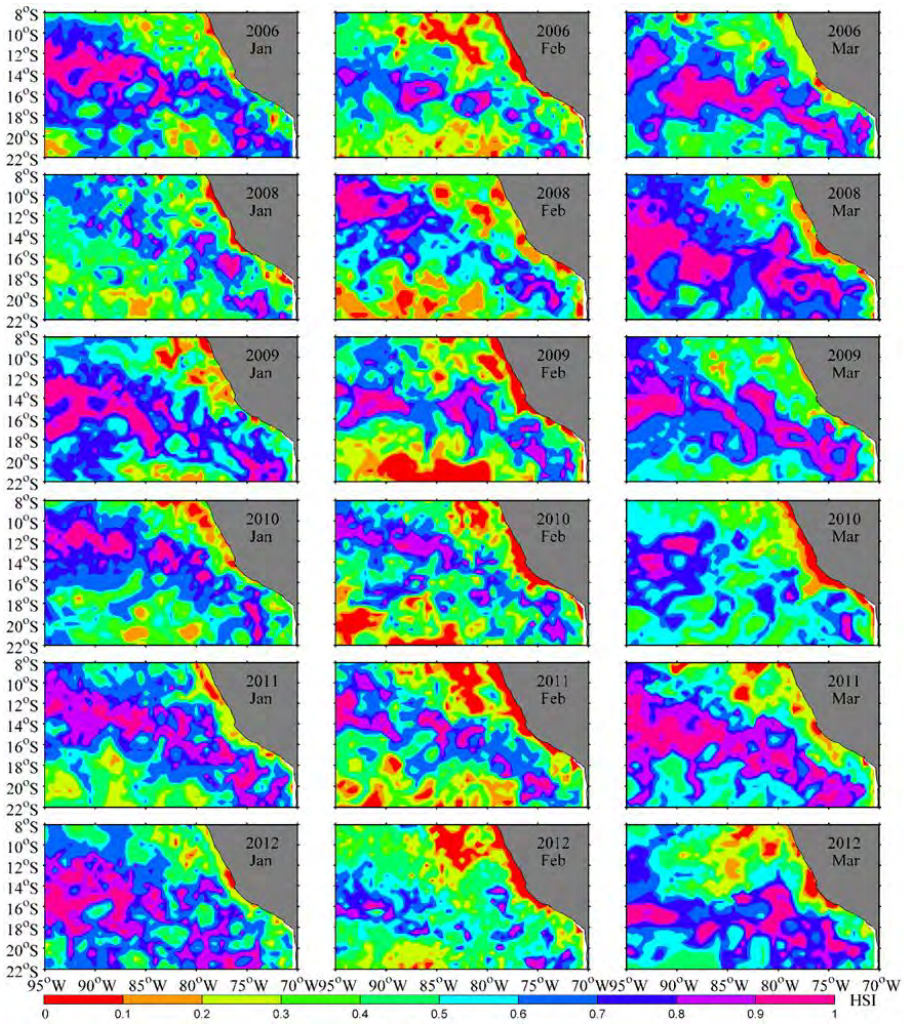

Figure 8. The spatial distribution of the predicted HSI values based on AMM-based HSI model from January to March in 2006 and 2008−2012.

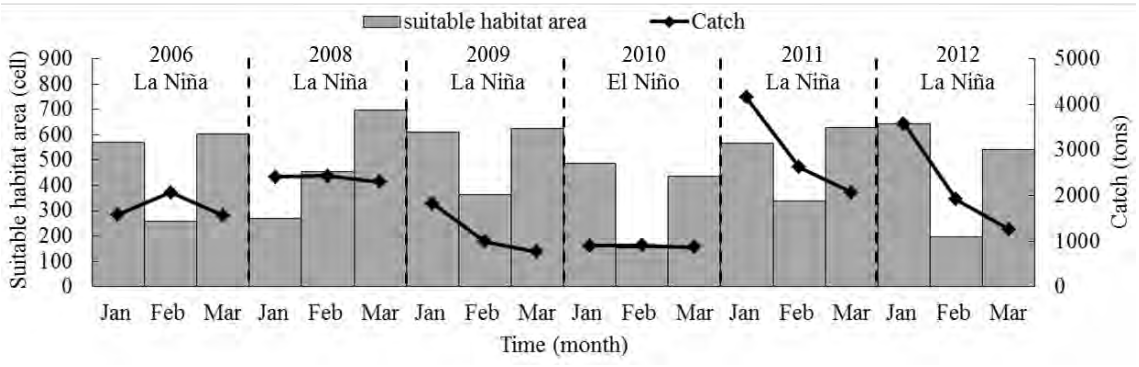

Figure 9. Suitable habitat area and catch from January to March in 2006 and 2008−2012.

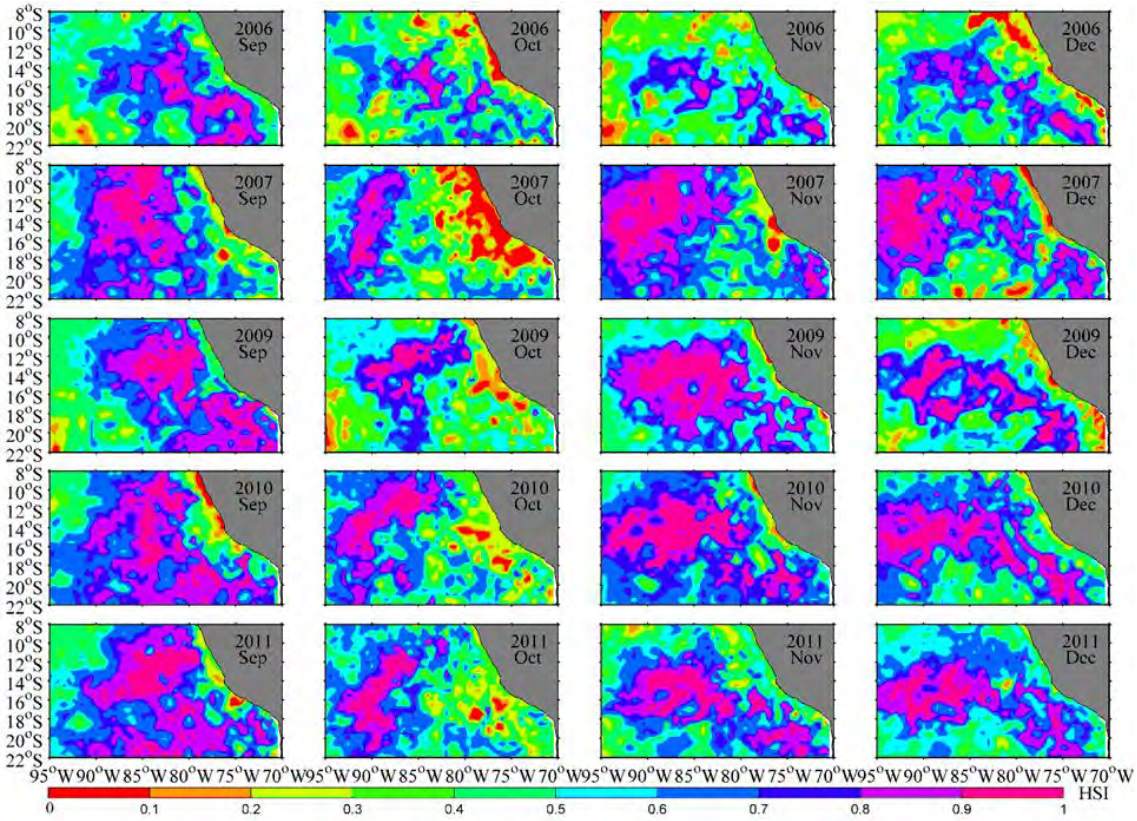

Figure 10. The spatial distribution of the predicted HSI values based on AMM-based HSI model from September to December in 2006, 2007 and 2009−2011.

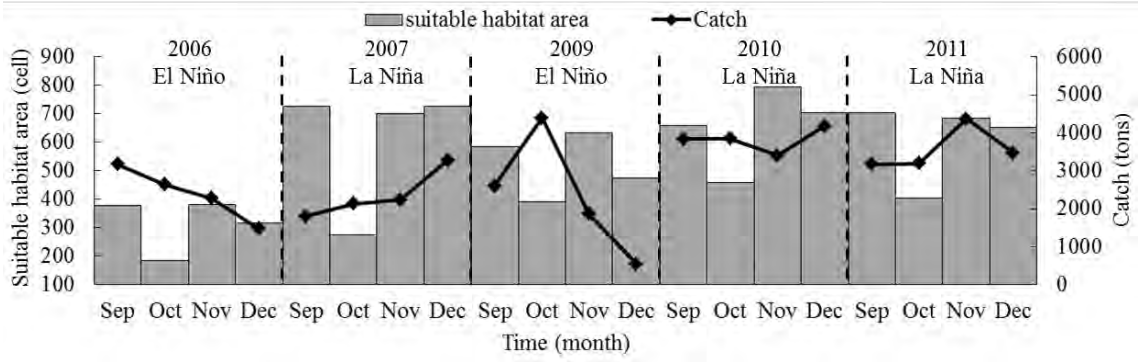

Figure 11. Suitable habitat area and catch from September to December in 2006, 2007 and 2009−2011.

The predicted suitable habitat during September to December tended to show a similar variability to the fishing months from January to March. It was clear that the La Niña events were likely to enlarge the suitable habitat in 2007, 2010 and 2011 for each month (Fig. 10), which ranged from 390 to 634 cells, from 460 to 794 cells and from 403 to 704 cells, respectively (Fig. 11). However, the habitat in 2006 and 2009 was affected by the El Niño events, resulting in a

significant decline of the areas of suitable habitat (Fig. 10), which fluctuated from 185 to 380 cells and from 275 to 726 cells, respectively (Fig. 11). Correspondingly, the La Niña events yielded a high squid catch in 2007, 2010 and 2011, especially in 2010 and 2011 but with a relatively low catch from September to November in 2007. Monthly catches in these years gradually increased and the highest catch was 4359 t in November 2011. On the contrary, the El Niño events in 2006 and 2009 were associated with poor catches with an exception in October 2009, the lowest catch was only 548 t in December 2009 (Fig. 11).

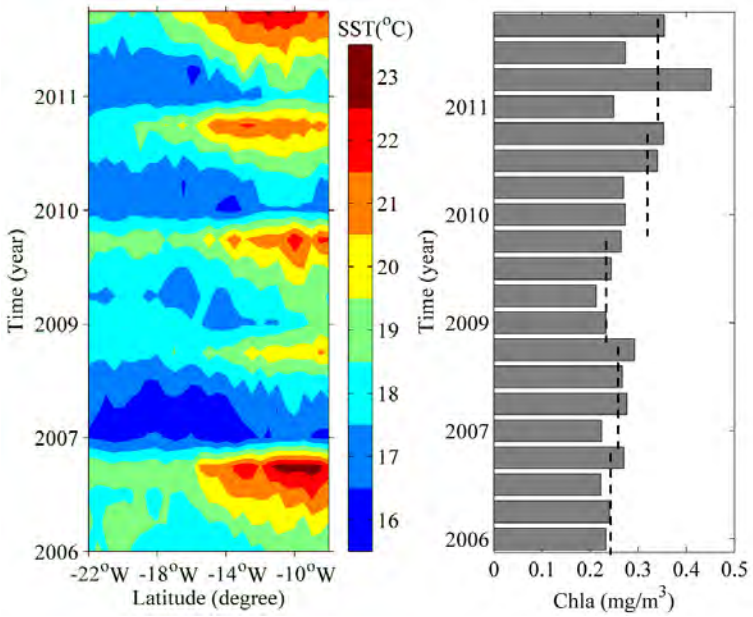

Figure 12. The left panel showed the time-longitude section of monthly SST on the fishing ground from September to December in 2006, 2007 and 2009−2011. The right panel denoted the monthly average Chla concentration from September to December in 2006, 2007 and 2009−2011. The black dashed line was the average Chla concentration for each year.

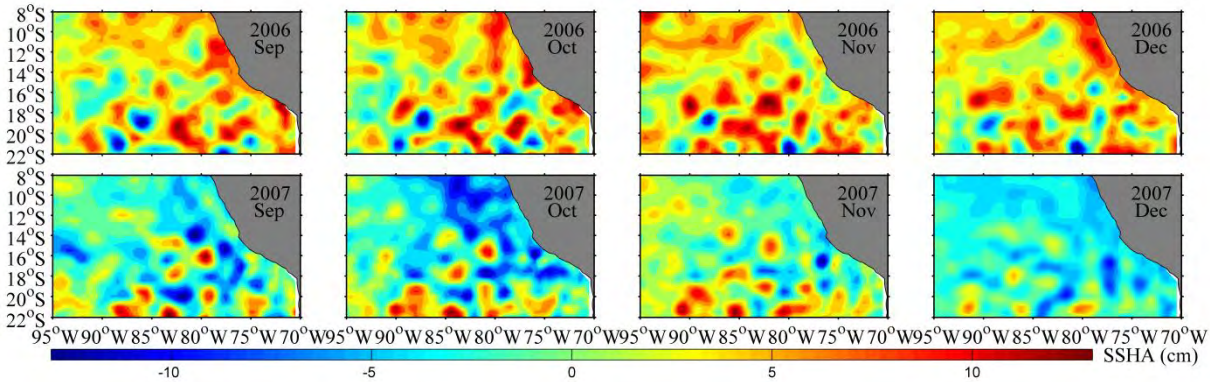

Figure 13. Comparing spatial distribution of SSHA on the fishing ground of *Dosidicus gigas* from September to December in 2006 and 2007

Outputs from the HSI model suggested that both suitable habitat areas and catches of D. gigas increased in La Niña periods and decreased in El Niño periods. This raised an interesting question how the critical environmental factors drove the variability in areas of squid suitable habitat during the year corresponding to an El Niño or a La Niña event? To address this question, we took the fishing months with high squid abundance from September to December for example to examine the variations in the environmental conditions in the years of 2006, 2007, 2009, 2010 and 2010. 2006 and 2009 were El Niño years, while 2007, 2010 and 2011 were La Niña years. We found that cold surface waters and high Chla extended to the entire fishing ground in the Southeast Pacific Ocean off Peru during 2007, 2010 and 2011, however, opposite patterns occurred in 2006 and 2009 (Fig. 12). Furthermore, the SSHA was elevated in 2006 but reduced in 2007 (Fig. 13). We merged these episodes into a picture to explore the potential mechanism that the large-scale climate variability influenced the squid habitat by changing the oceanographic processes in this study: the La Niña conditions resulted in strengthened upwelling coupling with cool and nutrient-enhanced waters, which yielded favorable habitat condition and high catch; whereas the El Niño conditions resulted in weaken upwelling coupling with warm and nutrient-depleted waters, which were unfavorable for the squid and reduced the catch..

References

Chang, Y. J., Sun, C. L., Chen, Y., Yeh, S. Z., DiNardo, G., and Su, N. J. 2013. Modelling the impacts of environmental variation on the habitat suitability of swordfish, *Xiphias gladius*, in the equatorial Atlantic Ocean. ICES Journal of Marine Science: Journal du Conseil, fss190.

Chen, X. J, Tian, S. Q., Chen, Y., and Liu, B. L. 2010. A modeling approach to identify optimal habitat and suitable fishing grounds for neon flying squid (*Ommastrephes bartramii*) in the Northwest Pacific Ocean. Fishery Bulletin, 108: 1-14.

Chen, X. J., Cao, J., Chen, Y., Liu, B. L., and Tian, S. Q. 2012. Effect of the Kuroshio on the spatial distribution of the red flying squid *Ommastrephes bartramii* in the Northwest Pacific Ocean. Bulletin of Marine Science, 88(1): 63-71.

Chen, X. J., Li, J. H., Liu, B. L., Li, G., and Lu, H. J. 2014. Fishery biology of jumbo flying squid *Dosidicus gigas* off Costa Rica Dome. Journal of Ocean University of China, 13(3): 485-490.

Chen, X. J., Liu, B. L., and Chen, Y. 2008a. A review of the development of Chinese distant-water squid jigging fisheries. Fisheries Research, 89(3): 211-221.

Keyl, F., Argüelles, J., and Tafur, R. 2010. Interannual variability in size structure, age, and growth of jumbo squid (*Dosidicus gigas*) assessed by modal progression analysis. ICES Journal of Marine Science: Journal du Conseil, fsq167.

Li, G., Chen, X. J., Lei, L., and Guan, W. J. 2014. Distribution of hotspots of chub mackerel based on remote-sensing data in coastal waters of China. International Journal of Remote Sensing, 35(11-12): 4399-4421.

Liu, B. L., Fang, Z., Chen, X. J., and Chen, Y. 2015. Spatial variations in beak structure to identify potentially geographic populations of *Dosidicus gigas* in the Eastern Pacific Ocean. Fisheries Research, 164: 185-192.

Morales-Bojórquez, E., and Nevárez-Martínez, M. O. 2010. Catch-at-size analysis for *Dosidicus gigas* in the central Gulf of California, Mexico in 1996–2002. Fisheries Research, 106(2): 214-221.

Nigmatullin, C. M., Nesis, K. N., and Arkhipkin, A. I. 2001. A review of the biology of the jumbo squid *Dosidicus gigas* (Cephalopoda: Ommastrephidae). Fisheries Research, 54(1): 9-19.

Postuma, F. A., and Gasalla, M. A. 2010. On the relationship between squid and the environment: artisanal jigging for Loligo plei at São Sebastião Island (24ºS), southeastern Brazil. ICES Journal of Marine Science: Journal du Conseil, fsq105.

Rocha, F., and Vega, M. A. 2003. Overview of cephalopod fisheries in Chilean waters. Fisheries Research, 60(1): 151-159.

Tian, S. Q., Chen, X. J., Chen, Y., Xu, L. X., and Dai, X. J. 2009. Evaluating habitat suitability indices derived from CPUE and fishing effort data for *Ommatrephes bartramii* in the northwestern Pacific Ocean. Fisheries Research, 95(2): 181-188.

Tomsic, C. A., Granata, T. C., Murphy, R. P., and Livchak, C. J. 2007. Using a coupled eco-hydrodynamic model to predict habitat for target species following dam removal. Ecological Engineering, 30(3): 215-230.

Yu, W., Chen, X. J., Yi, Q., Chen, Y., and Zhang, Y. 2015. Variability of suitable habitat of western winter-Spring cohort for neon flying squid in the Northwest Pacific under anomalous environments. PloS one, 10(4).